# A.c. and d.c. conduction processes in octakis[(4-tert-butylbenzylthio)-porphyrazinato]Cu(II) thin films with gold electrodes

**BAHADIR KESKIN, AHMET ALTINDAL[†,*], ULVI AVCIATA[†] and AHMET GÜL[††]**

Department of Chemistry, Yildiz Technical University, 34210 Istanbul, Turkey
[†]Department of Physics, Yildiz Technical University, 34210 Istanbul, Turkey
[††]Department of Chemistry, Istanbul Technical University, 34469 Maslak, Istanbul, Turkey

**Abstract.** The d.c. and a.c. electrical transport properties of Au/Pz/Au devices with various thickness of Pz(octakis[(4-tert-butylbenzylthio)-porphyrazinato]Cu(II)) layer have been investigated. Measurements revealed that, in contrast to previously investigated Au/Pc/Au structures, low voltage d.c. behaviour of the films can be described by the field-lowering mechanisms with a $\log(J) \propto V^{1/2}$ current density-voltage characteristics under forward and reverse bias. For high reverse voltages, the observed $\ln(J/V^2) - 1/V$ characteristics indicated that the origin of conduction mechanism is Fowler–Nordheim tunnelling (FNT). On the other hand, the voltage dependence of current density at the higher forward-voltage region indicates that the mechanism of conduction in Au/Pz/Au devices is space charge limited conduction dominated by exponential trap distribution. A thickness independent barrier height was observed for tunnelling, while the total trap concentration show a general tendency to decrease with increasing film thickness. The a.c. conductivity showed two regions in the $\ln(\sigma_{a.c.}) - \ln(f)$ plots having different slopes, leading to the conclusion that for low frequency region, the dominant conduction mechanism is a small polaron tunnelling at all temperatures, whereas for high frequency region, correlated barrier hopping model is the dominant mechanism in the investigated devices.

**Keywords.** Porphyrazine; a.c. conductivity; correlated barrier hopping; spin coating; tunnelling.

## 1. Introduction

With the rising interest in organic electronics, tetrapyrrolicmacrocycles such as porphyrins, phthalocyanines and porphyrazines have attracted much interest due to their potential in technological applications. In particular, phthalocyanines and porphyrins are especially attractive because of their unique chemical and physical properties that make them ideal candidates for developing photonic and electronic devices (Mckeown 1989; Jin *et al* 2003; Campbell*et al* 2004; Salan *et al* 2012), optical limiter (Gould 1996; Hanack *et al* 2001; Calvete*et al* 2004) and gas sensors (Newton *et al* 2000; Sülü *et al* 2005; Odabas *et al* 2010). Although structurally porphyrazines have been related to phthalocyanines more close lythan to porphyrins, porphyrazines have received considerably lesser interest than the related phthalocyanines. On the other hand, intensive research on peripherally functionalized porphyrazines during the last decadehas shown that these tetrapyrrole derivatives shouldbe considered as alternatives to the phthalocyanines (Polat and Gül 2000).

For most applications, an understanding of the charge transport properties of both a.c. and d.c. conditions are crucial in order to realize its future applications. Therefore, the extraction of true intrinsic nature of electrical conduction mechanism play an important role and these are often the deciding factors about the suitability of the material for a particular device application and optimization. a.c. and d.c. electrical properties of many phthalocyanines have been studied in detail by several authors in the form of both single crystal and thin film (Öztürk *et al* 1992; Shafai and Anthopoulos 2001; Altındal *et al* 2005). Unlike some phthalocyanines, the electronic properties and the dependence of transport processes on the film thickness of porphyrazines have not been reported to the best of our knowledge.

In the present work, we have investigated the d.c. and a.c. transport properties of [octakis(4-tert-butylbenzylthio) porphyrazinato]Cu(II) thin films by analysing the current density–voltage (*J–V*) and a.c. conductivity-frequency ($\sigma_{a.c.} - f$) characteristics, respectively. We have shown that the measured current in Au/Pz/Au device is field-lowering mechanisms for low applied voltages. The current becomes space charge limited at high-forward voltages and tunnelling contributes significantly to charge injection for reverse bias. The temperature and frequency dependent conductivity are well-analysed by small polaron tunnelling at low frequency and correlated barrier hopping at high frequency.

*Author for correspondence (altindal@yildiz.edu.tr)

## 2.  Experimental

The devices were fabricated on ordinary glass substrates. The glass substrates were cleaned by ultrasonic treatment in acetone, isopropyl alcohol and deionized water before insertion into the deposition chamber. After surface cleaning, Au metal with high purity (99·99%) was thermally evaporated on the substrate at a pressure of $1 \times 10^{-5}$ mbar in thermal evaporation system (Edwards Auto 500). The synthesis procedure of octakis(4-tert-butylbenzylthio) porphyrazinato] Cu(II) molecule, shown in scheme 1 was described in (Keskin *et al* 2008). TLC, elemental analysis and NMR spectra showed clearly that the compound was sufficiently pure. Pz thin films with different thickness between 200 and 400 nm were deposited on the Au coated glass substrate by a spin coating method at 1500 rpm using DMF as solvent. An elipsometric technique was used to measure the thickness of Pz films. The error in the measurement of the thickness of Pz films is estimated at about 1%. Subsequently, the films were thermally annealed at 120 °C for 45 min to evaporate the solvent. After spinning process, circular dots of 1 mm in diameter and 2000 Å thickness Au contact were deposited on the top of Pz layer through a metal shadow mask in a high vacuum system in the pressure of $1 \times 10^{-5}$ mbar. The current–voltage (I–V) measurements on Au/Pz/Au

sandwich structure were performed using a Keithley 6517A electrometer. The a.c. conductivity and impedance measurements were carried out with an Agilent 4284A LCR meter in the frequency range, $20–2 \times 10^{6}$ Hz and in the temperature range from 300 to 450 K. The temperature of each sample was determined during the measurements using a pre-calibrated *K*-type thermocouple with an error of $\pm 0.1$ K. All measurements were performed under vacuum ($\leq 10^{-3}$ mbar) in the dark, but the values did not change under illumination with the indoor lighting. Both the d.c. conductivity and impedance data were recorded on a PC using a GPIB data transfer card. The results obtained under these conditions were reproducible with an uncertainty $< 4\%$.

## 3.  Results and discussion

### 3.1  *d.c. conductivity*

In order to gain insight into the charge transport mechanism in Pz film, the *J–V* characteristics for Au/Pz/Au devices with Pz thickness of 200, 250, 310, 350 and 400 nm are measured and displayed in the log–log scale in figure 1. The general behaviour of current density is the presence of two regions in (log *J* vs log *V*) relation, one at
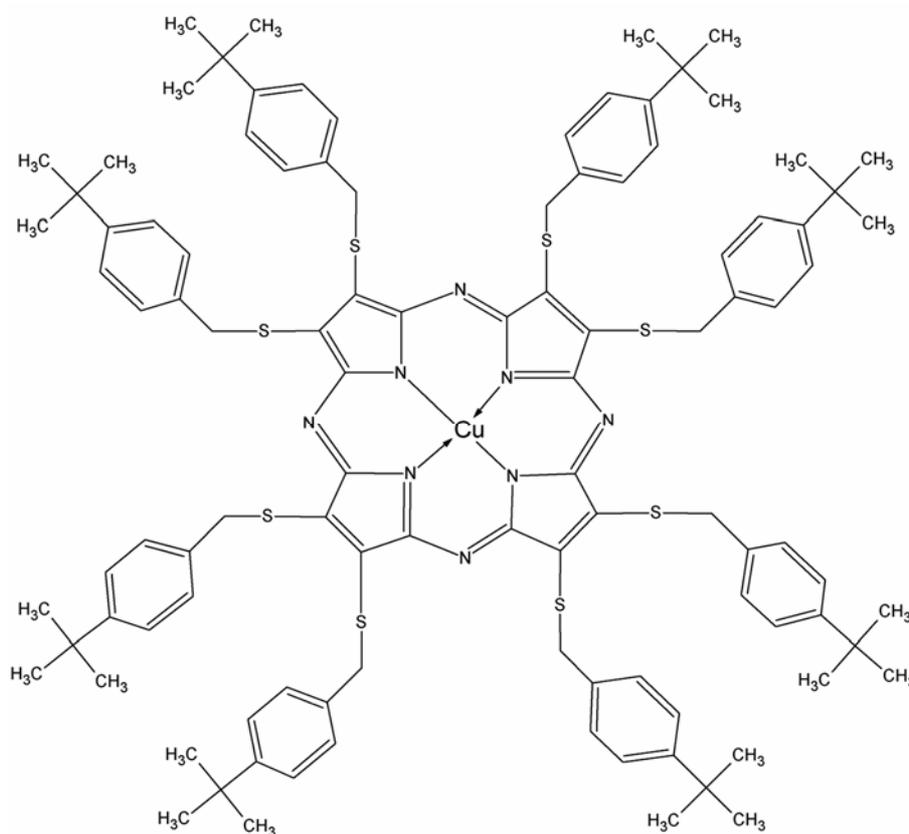


**Scheme 1.**    Octakis [(4-tert-butylbenzylthio) porphyrazinato]Cu(II).

relatively low voltage, while the other appears at high voltage. The change in these two regions is linear and are characterized by two different conduction mechanisms operating in the device depending on the applied voltage. This type of *J–V* characteristics have been extensively observed in Au/H$_2$Pc/Au (Amar *et al* 1998), Au/CoPc/Au (Abdel Malik andAbdel-Latif 1997) and Au/MgPc/Al (Varghese and Menon 2006a, b) structures over the last two decades, and recently have also been observed in Au/zinc phthalocyanine doped with tetrafluorotetracyanoquinodimethane/Au (Gao and Kahn 2002) devices. In all of these reports, a linear dependence of *J* on *V* with a slope of unity at lower voltages and a power law ($J \propto V^m$) with $m > 2$ dependence at higher voltages have been observed, which is indicative of space charge limited conductivity (SCLC) controlled by exponentially distributed trapping levels.

Various conduction processes such as space charge limited conductivity (SCLC), field-lowering mechanisms (Schottky and Poole–Frenkel effects) and Fowler–Nordheim tunnelling (FNT) have been identified for the charge transfer mechanism in organic materials.

As can be seen from figure 1 that, in our case, the forward-bias current density increases very slowly with voltage up to certain value of applied voltage, above which the increase is more rapid. It was found that the slope of the double logarithmic *J–V* plots vary between 0·35 and 0·51 at lower voltages. The lower voltage region can no longer be treated as ohmic, as the slope is between 0·35 and 0·51. A similar trend is apparent for reverse bias, where the slopes are ~ 0·45 in the lower voltage region. The observed low voltage *J–V* characteristic is therefore in marked contrast to those observed in the above mentioned work and analysed in terms of the two



**Figure 1.** Thickness dependence of forward bias *J–V* characteristics for Au/Pz/Au device at room temperature.

field-lowering mechanisms. In the case of field-lowering mechanisms, current density expressions are given by (Simmons 1971):

$$J = A^* T^2 \exp\left(-\frac{\phi_s}{kT}\right)\exp\left(\frac{\beta_s}{kT}\sqrt{\frac{V}{d}}\right), \tag{1}$$

for the Schottky effect and by

$$J = J_0 \exp\left(\frac{\beta_{PF}}{kT}\sqrt{\frac{V}{d}}\right), \tag{2}$$

for the Poole-Frenkel effect, where $A^*$ is the Richardson constant, $\phi_s$ is the Schottky barrier height at the injecting electrode interface, $k$ is the Boltzmann constant, $d$ is the film thickness, $T$ is the temperature, $\beta_s$ and $\beta_{PF}$ are the Schottky and Poole–Frenkel field-lowering coefficients, respectively and $J_0$ is the low field current density. These two field-lowering coefficients are related by:

$$2\beta_s = \beta_{PF} = \left(\frac{e^3}{2\pi\varepsilon\varepsilon_0}\right)^{1/2}, \tag{3}$$

where $e$ is the electronic charge, $\varepsilon$ the relative permittivity of the material and $\varepsilon_0$ the permittivity of free space. In order to determine $\varepsilon$ value for the investigated Pz film, the capacitance of the samples with various thickness of Pz layer was measured at a frequency of 1 kHz. A linear dependence of the capacitance $C$ on inverse thickness was observed, implying that $\varepsilon$ value can be determined by the geometric capacitance expression $C = \varepsilon\varepsilon_0 A/d$. A permittivity value of $3\cdot75 \times 10^{-11}$ F m$^{-1}$ ($\varepsilon = 4\cdot24$) was derived and this value is used in the analysis of the obtained data. It is evident from (1) and (2) that by plotting ln ($J$) vs $V^{1/2}$, the value of $\beta$ can be determined. Such a plot is shown in figures 2(a) and (b) for the forward- and reverse-bias characteristics, respectively. It is clear from figure 2 that there are two linear regions in both the cases.

The values of $\beta$ calculated from the slope of the lower voltage section of figure 2 and derived values of $\beta$ for forward and reverse bias voltages are summarized in table 1. The theoretical values of $\beta_{PF}$ and $\beta_s$ were determined using (3) and were found as $2\cdot60 \times 10^{-5}$ eVm$^{1/2}$ V$^{-1/2}$ and $1\cdot30 \times 10^{-5}$ eVm$^{1/2}$ V$^{-1/2}$, respectively.

The average $\beta_{PF}$ and $\beta_s$ values for forward and reverse bias were determined from experimental data and were found as $\beta_{Pfav} = 3\cdot90 \times 10^{-5}$ for forward bias, $\beta_{Pfav} = 2\cdot26 \times 10^{-5}$ for reverse bias, $\beta_{sav} = 1\cdot96 \times 10^{-5}$ for forward bias and $\beta_{sav} = 1\cdot13 \times 10^{-5}$ eV m$^{1/2}$ V$^{-1/2}$ for reverse bias. The results showed that the average $\beta$ experimental value is closely related to the theoretical value of $\beta_s$. This suggests that Schottky-type conduction is dominant at lower applied voltages in both directions.

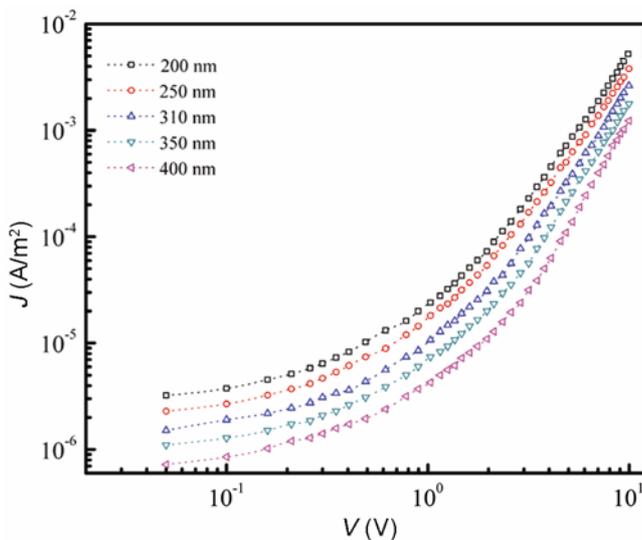The values of the power law exponent, $m$, has been calculated from the slope of log *J* vs log *V* graphs for higher

**Table 1.** Summary of field-lowering mechanism parameters.

| Thickness (nm) | $\beta_{PF}$ (eV m$^{1/2}$ V$^{-1/2}$) | | $\beta_s$ (eV m$^{1/2}$ V$^{-1/2}$) | |
| | Forward | Reverse | Forward | Reverse |
| --- | --- | --- | --- | --- |
| 200 | $3.33 \times 10^{-5}$ | $1.83 \times 10^{-5}$ | $1.66 \times 10^{-5}$ | $9.15 \times 10^{-6}$ |
| 250 | $3.66 \times 10^{-5}$ | $2.00 \times 10^{-5}$ | $1.83 \times 10^{-5}$ | $1.00 \times 10^{-5}$ |
| 310 | $4.04 \times 10^{-5}$ | $2.30 \times 10^{-5}$ | $2.02 \times 10^{-5}$ | $1.15 \times 10^{-5}$ |
| 350 | $4.23 \times 10^{-5}$ | $2.51 \times 10^{-5}$ | $2.12 \times 10^{-5}$ | $1.25 \times 10^{-5}$ |
| 400 | $4.30 \times 10^{-5}$ | $2.68 \times 10^{-5}$ | $2.15 \times 10^{-5}$ | $1.34 \times 10^{-5}$ |
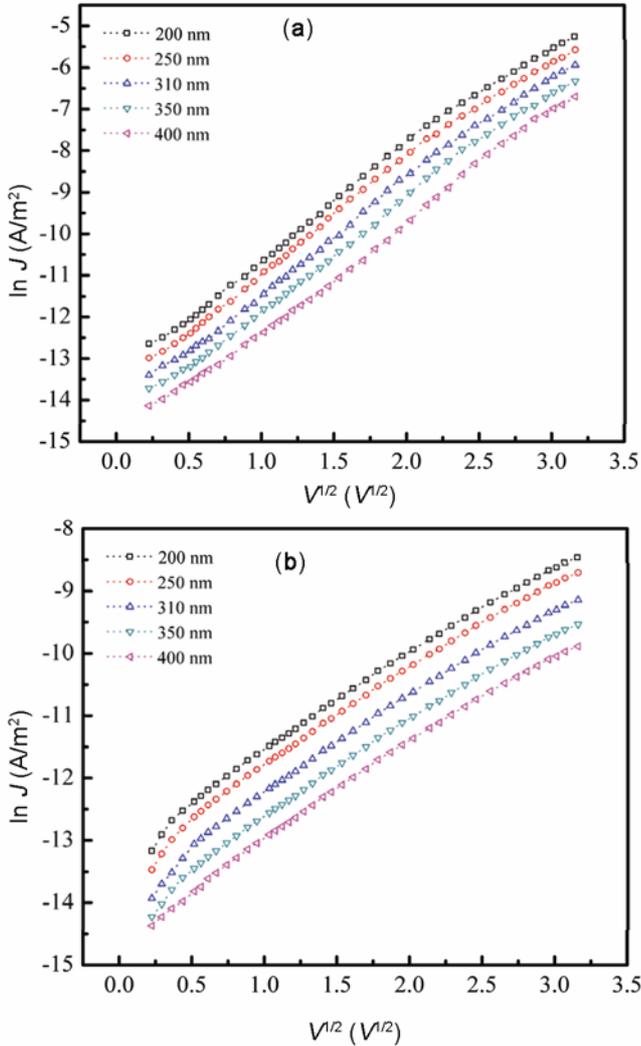


**Figure 2.** Plots of $\ln J$ vs $V^{1/2}$ of Au/Pz/Au device in forward (**a**) and reverse (**b**) directions at various thicknesses of Pz.

applied voltages. Our calculations showed that $m$ is thickness independent ($m = 1.52$) for reverse bias direction. On the other hand, it was found that $m$ is definitely a function of film thickness for forward bias direction and shows a general tendency to increase with increasing film thickness (figure 3). It can be seen from figure 3, that the exponent $m$ is always $> 2$ for forward direction. The ex-

tracted values of the power law exponent suggests that the conduction processes through Au/Pz/Au devices cannot be discussed in terms of space charge limited conductivity for reverse bias, while for forward direction space-charge limited process controlled by an exponential distribution of trapping levels is the dominant conduction processes.

Another conduction mechanism commonly used is Fowler–Nordheim tunnelling. The basic idea of Fowler–Nordheim tunnelling, which is a quantum mechanical phenomenon, is that quantum tunnelling of electrons with insufficient energy occurs through a triangular potential barrier into the conduction band of an oxide. If the mechanism responsible for conduction can be considered as FNT, the current density attributed to FNT can be described as given in (Schroder 1998).

$$J = \frac{A}{4\phi_B} E^2 \exp\left( -\frac{2B\phi_B^{3/2}}{E} \right), \tag{4}$$

where $J$, $E$ and $\phi_B$ are current density, electrical field, potential barrier height at the metal-film interface, respectively and $A$ and $B$ are constants.

According to (4), since $A$ and $B$ are independent from the electric field, the slope of $\ln(J/E^2)$ vs $1/E$ graph should be constant. In order to examine whether our high voltage data can be explained using Fowler–Nordheim tunnelling model, we have plotted, in figure 4, $(J/V^2)$ vs $1/V$ curves for both reverse and forward directions in a semi-logarithmic scale for the device with 200 nm Pz film (the same type of characteristics were observed for other films). With the examination of the reported experimental data (figure 4) clear differences could be seen in the dependence of $(J/V^2)$ on $1/V$ for reverse and forward bias conditions. As can be seen clearly from figure 4 that $\ln(J/V^2) - 1/V$ curve for reverse bias represents a straight line (having a linearity factor $> 0.99$), of negative slope, as predicted by the Fowler–Nordheim expression for tunnelling. The observed $\ln(J/V^2) - 1/V$ characteristics with thickness independent slopes suggest that the origin of conduction mechanism is FNT at high reverse bias which is clearly not the case for forward direction.

With the aid of (4), the value of the barrier height, $\phi_B$, has been calculated from the slope of $\ln(J/V^2)$ vs $1/V$

graphs. After taking a value of the tunnelling thickness $d_t = 5$ nm, the value of the barrier height was estimated and found to be 0·26 eV at room temperature. The obtained value of $\phi_B$ is comparable to those usually found for organic films, such as copper phthalocyanine (Hassan and Gould 1989).

As been mentioned earlier, *I–V* curves can be characterized by a power law dependence in the form $J \propto V^m$ at higher applied forward bias voltages. This type of *J–V* characteristic has been reported by several workers for Pc film such as, CuPc (Hassan and Gould 1989) and PbPc (Ray *et al* 1999). It has been demonstrated by Simmons (1971) that the numerical value of the index *m* is
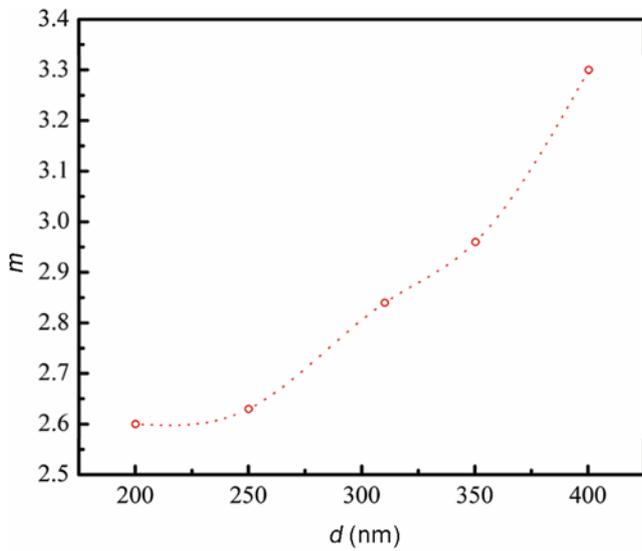


**Figure 3.** Variation of power law exponent, *m*, as a function of film thickness at room temperature.
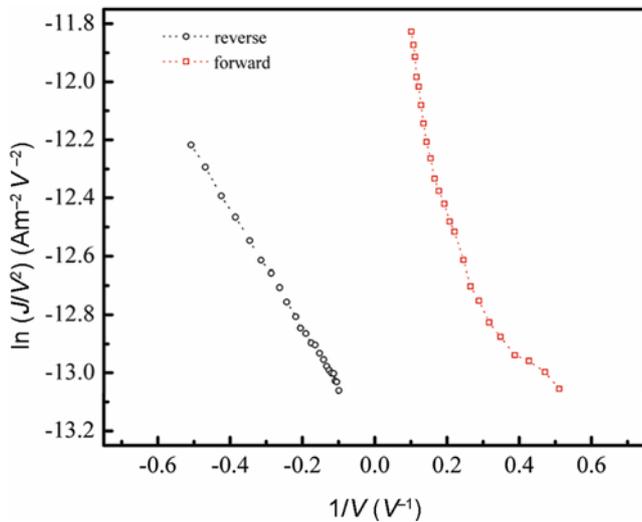


**Figure 4.** Fowler–Nordheim plot [ln($J/V^2$) – 1/V] of Au/Pz (200 nm)/Au device under reverse and forward applied voltages.

associated with the nature of traps and their distribution within the forbidden gap. The power-law dependence between current and voltage with $m \geq 2$ is described in terms of a space-charge limited process controlled by a single dominant trap level ($m = 2$) and an exponential distribution of trapping levels ($m > 2$), respectively. Following Lampert (1964), *J–V* dependence is given for $m = 2$ by:

$$J = \frac{9}{8}\varepsilon\mu\theta\left(\frac{V^2}{d^3}\right),\tag{5}$$

and for $m > 2$ by:

$$J = e\mu N_v\left(\frac{\varepsilon}{ekP_0T_t}\right)^l \frac{V^{l+1}}{d^{2l+1}},\tag{6}$$

where $\varepsilon$ is the permittivity of the film, $\mu$ is the mobility of the carriers, *V* is the applied voltage, *d* is the thickness of Pz film, $\theta$ is the ratio of free charge carriers to the trapped carriers, $N_v$ is the effective density of states in the valence band and *k* is the Boltzmann constant. $P_0$ is the trap density per unit energy range at the valence band edge and $l = m - 1$ is the ratio $T_t/T$ where *T* is the absolute temperature. $T_t$ is a temperature parameter which characterizes the exponential trap distribution such that:

$$P(E) = P_0 \exp\left(-\frac{E}{kT}\right),\tag{7}$$

where $P(E)$ is the trap density per unit energy range at an energy *E* above the valence band edge and $P_0$ is the value of $P(E)$ at the valence band edge. The total trap concentration $N_t$, is given as (Gould and Rahman 1981)

$$N_t = P_0 kT_t,\tag{8}$$

Taking a typical value of the mobility in organic semiconductor $\mu = 4 \times 10^{-6}$ m$^2$ V$^{-1}$ s$^{-1}$ and $N_v = 10^{27}$ m$^{-3}$ (Sussman 1967) and using (6) and (8), the value of $P_0$ and $N_t$ were determined. Derived results for $P_0$, $T_t$ and $N_t$ are summarized in table 2. It was observed that the obtained $N_t$ values for the studied diode are higher than that of NiPc thin films using gold and lead electrodes ($N_t = 2\cdot53 \times 10^{22}$ m$^{-3}$) (Varghese and Menon 2006a, b) and Au/ZnPc/Au device ($N_t = 8\cdot34 \times 10^{24}$ m$^{-3}$) (Zeyada and El-Nahass 2008). It is well known that native defects,

**Table 2.** Electrical parameters in SCLC region of Au/Pz/Au device.

| Thickness (nm) | $T_t$ (K) | $P_0$ (J$^{-1}$ m$^{-3}$) | $N_t$ (m$^{-3}$) |
|---|---|---|---|
| 200 | 480 | $8\cdot6 \times 10^{48}$ | $5\cdot6 \times 10^{28}$ |
| 250 | 489 | $4\cdot0 \times 10^{48}$ | $2\cdot7 \times 10^{28}$ |
| 310 | 552 | $3\cdot2 \times 10^{47}$ | $2\cdot4 \times 10^{28}$ |
| 350 | 588 | $9\cdot6 \times 10^{44}$ | $7\cdot8 \times 10^{26}$ |
| 400 | 690 | $3\cdot5 \times 10^{44}$ | $3\cdot3 \times 10^{24}$ |

which act as either trapping or recombination centres, and their concentration is dependent on the film preparation conditions and play an important role in determination of conduction mechanism in the films. It is also well established that oxygen is known to act as an acceptor centre for most organic compound. We believe that the observed high value of $N_t$ is mostly due to the traps generated by oxygen diffusion from the outer environment. In this sense, oxygen acts as an acceptor centre and trapping of holes near $O_2$ ions may occur, thus contributing to the measured value of $N_t$. After oxygen doping an increase in $N_t$ value for Au/NiPc/Al device was also reported by Anthopoulos and Shafai (2003). As can be seen from table 2, value of the total trap concentration decreases with increasing film thickness. It is widely believed that with increasing disorder the density of traps increases and a completely disordered structure may have an unlimited number of localized levels. Therefore, the increase in $N_t$ is attributed to the increase of Pz crystallite size with increasing the film thickness (Hassan *et al* 1996).

### 3.2 *a.c. conductivity*

Figure 5 presents a.c. response for a range of measurement frequencies (20 Hz–2 MHz) for Au/Pz/Au devices with various Pz thickness at room temperature. It is clear that $\ln(\sigma_{a.c.}) - \ln(f)$ characteristics exhibit two regions for all thickness. In the lower frequency region (20 Hz–1500 Hz), the a.c. conductivity exhibits relatively weak dependence on frequency, whereas at higher frequencies (1500 Hz–2 MHz) a strong frequency dependence with a slope of approximate unity. A considerable number of experimental data concerning the frequency dependent conductivity of large variety of materials such as



**Figure 5.** Dependence of a.c. conductivity on frequency at room temperature.

covalent or ionic bonded amorphous solids, molecular materials have been accumulated which obey a power law given by

$$\sigma(\omega) = \sigma_0 \omega^s, \tag{9}$$

where $\omega$ is the angular frequency, $\sigma_0$ and $s$ have usually been found to be temperature dependent parameters. To describe the charge transfer mechanism in the materials containing both amorphous and crystalline phases, different theoretical models such as quantum mechanical tunnelling (QMT), correlated barrier hopping (CBH) have been proposed. It is difficult to decide which mechanism is responsible for the conductivities of the investigated compounds. In these models, the frequency exponent, $s$, has different trends in terms of its dependence on temperature and frequency (Elliot 1987). QMT model assumes that carrier motion occurs through quantum mechanical tunnelling between localized states near the Fermi level. This model predicts a temperature independent $s$ value which is given by

$$s = 1 + \frac{4}{\ln(\omega \tau_0)}, \tag{10}$$

where $\tau_0$ is the characteristic relaxation time of the carrier. On the other hand, hopping model, which was developed by Pollak and Geballe (1961), assumes that charge carriers hop between sites over the potential barrier separating them, rather than tunnelling through the barrier. This model, in contrary to QMT model, predicts a temperature-dependent $s$ which increases with decreasing temperature. The temperature dependent frequency exponent, $s$, for hopping model is given by

$$s = 1 - \frac{6kT}{W_M}, \tag{11}$$

where $W_M$ is the optical bandgap, $k$ is the Boltzmann constant and $T$ is the temperature.

To investigate the conduction mechanism involved the variation of the frequency exponent, $s$, with temperature were examined. Values of $s$ were calculated from the straight line fits in $\ln(\sigma_{a.c.})$ vs $\ln(f)$ graphs for each frequency regions. The temperature dependence of the extracted values of $s$ for Au/Pz (250 nm)/Au structure is shown in figure 6 for both low and high frequency regions. Our calculations showed that the exponent, $s$, increases with increasing temperature for low frequency region, while it decreases with increasing temperature for high frequency region. As can be seen from figure 6, high frequency value of s is very close to unity at room temperature, while low frequency value of $s$ is $< 1$. In view of the above mentioned models, the present investigation leads to the following inferences: (i) According to small polaron quantum mechanical tunnelling model, the exponent, $s$, is an increasing function of temperature (Long
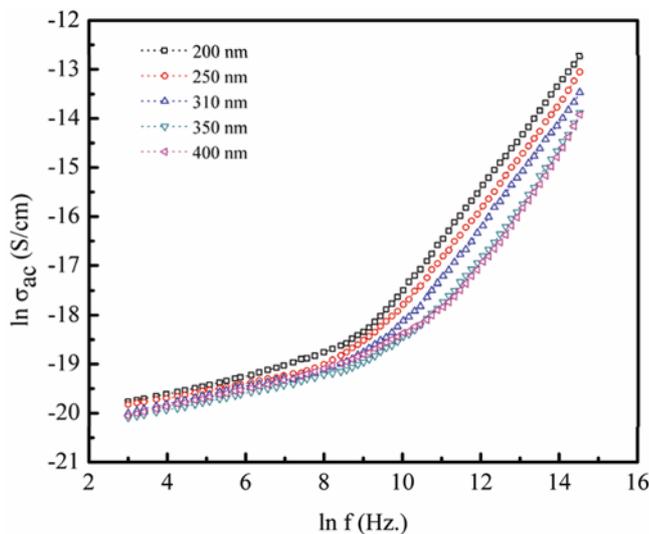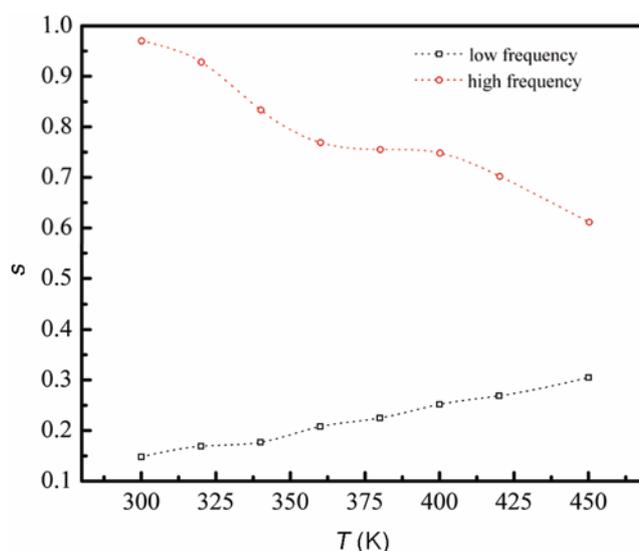
**Figure 6.** Variation of frequency exponent, *s* vs temperature for low and high frequencies.

1982). Therefore, it can be concluded that for the low frequency region, the low values of *s* and its temperature dependence indicate that the dominant conduction mechanism in Au/Pz/Au structures are small polaron tunnelling and (ii) on the other hand, our a.c. analysis based on the existing theories showed that the temperature dependence of the frequency exponent, *s*, is in good agreement with CBH model predictions for all the samples investigated.

## 4. Conclusions

Au/Pz/Au structures were prepared and their electronic properties under d.c. and a.c. conditions were studied. From the detailed analysis of the current density–voltage measurements, it has been observed that the Schottky-type conduction is dominant at lower applied voltages in both directions. A slope > 2 in the high forward-bias region confirm SCLC governed by the exponential trap distribution, whereas at high reverse bias, the transport is dominated by tunnelling. It was also observed that the conduction mechanism for both directions is independent of the film thickness. Total trap concentration, $N_t$, has been calculated and it was found that $N_t$ decreases with increasing film thickness. This behaviour was attributed to the increase of the Pz crystallite size with increasing film thickness. Frequency and temperature dependence of the a.c. conductivity have been analysed in terms of QMT and CBH models. Based on the existing theories of a.c. conduction, we have found no results supporting the QMT model. The temperature dependence of the exponent, *s*, seems to support the small polaron tunnelling at low frequency and CBH model at high frequency region. In summary, more work on CuPz thin films are essential

to the better understanding of such systems. The work should concentrate on the variation of d.c. and a.c. electrical properties and dielectric behaviour with film preparation method and conditions, heat treatment, annealing duration and atmosphere (especially the effect of oxygen), the effect of electrode material and substrate.

## References

Abdel Malik T G and Abdel-Latif R M 1997 *Thin Solid Films* **305** 336
Altındal A, Abdurrahmanoğlu Ş, Bulut M and Bekaroğlu Ö 2005 *Synth. Met.* **150** 181
Amar N, Gould R D and Saleh A M 1998 *Vacuum* **50** 53
Anthopoulos T D and Shafai T S 2003 *J. Phys. Chem. Solids* **64** 1217
Calvete M, Yang G Y and Hanack M 2004 *Synth. Met.* **141** 231
Campbell W M, Burrell A K, Officer D L and Jolley K W 2004 *Coord. Chem. Rev.* **248** 1363
Elliot S R 1987 *Adv. Phys.* **36** 135
Gao W and Kahn A 2002 *Org. Electron.* **3** 53
Gould R D and Rahman M S 1981 *J. Phys. D: Appl. Phys.* **14** 79
Gould R D 1996 *Coord. Chem. Rev.* **156** 237
Hanack M, Schneider T, Barthel M, Shirk J S, Flom S R and Pong R G S 2001 *Coord. Chem. Rev.* **219** 235

Hassan A K and Gould R D 1989 *J. Phys. D: Appl. Phys.* **22** 1162

Hassan A K, Gould R D and Ray A K 1996 *Phys. Stat. Sol. (a)* **158** K23

Jin R C, Cao Y C, Hao E C, Metraux G S, Schatz G C and Mirkin C A 2003 *Nature* **425** 487

Keskin B, Köseoğlu Y, Avcıata U and Gül A 2008 *Polyhedron* **27** 1155

Lampert M A 1964 *Rep. Prog. Phys.* **27** 329

Long A R 1982 *Adv. Phys.* **31** 553

Mckeown N B 1989 *Phthalocyanine materials synthesis, structure and function* (Cambridge: Cambridge University Press)

Newton M I, Starkea T K H, Willis M R and McHale G 2000 *Sens. Actuators* **B67** 307

Odabas Z, Altındal A, Özkaya A R, Salih B and Bekaroğlu Ö 2010 *Sens. Actuators* **B145** 355

Öztürk Z Z, Altındal A, Gürek A and Bekaroğlu Ö 1992 *Synth. Met.* **52** 291

Polat M and Gül A 2000 *Dyes Pigments* **45** 195

Pollak M and Geballe T H 1961 *Phys. Rev.* **122** 1742

Ray A K, Traceyand S M and Hassan A K 1999 *IEEE Proc. Sci. Meas. Technol.* **146** 205

Salan Ü, Altındal A, Özkaya A R, Salih B and Bekaroğlu O 2012 *Dalton Trans.* **41** 5177

Schroder DK 1998 *Semiconductor material and device characterization* (New York: Wiley) pp. 368–387

Shafai T S and Anthopoulos T D 2001 *Thin Solid Films* **398** 361

Simmons J G 1971 *J. Phys. D: Appl. Phys.* **4** 613

Sülü M, Altındal A and Bekaroğlu Ö 2005 *Synth. Met.* **155** 211

Sussman A 1967 *J. Appl. Phys.* **38** 2738

Varghese A C and Menon C S 2006a *J. Mater. Sci: Mater Electron.* **17** 149

Varghese A C and Menon C S 2006b *Centr. Eur. J. Phys.* **4** 20

Zeyada H M and El-Nahass M M 2008 *Appl. Surf. Sci.* **254** 1852